ESD-TR-77-224

Technical Note	1977-19
Spatial Acquisition in Optical Space Communications	A. A. Braga-Illa H. M. Heggestad E. V. Hoversten J. T. Lynch 6 September 1977

Lincoln Laboratory

MASSACHUSETTS INSTITUTE OF TECHNOLOGY

LEXINGTON, MASSACHUSETTS

ADA046581

MASSACHUSETTS INSTITUTE OF TECHNOLOGY

LINCOLN LABORATORY

SPATIAL ACQUISITION IN OPTICAL SPACE COMMUNICATIONS

A. A. BRAGA-ILLA
H. M. HEGGESTAD
E. V. HOVERSTEN
J. T. LYNCH

Group 66

TECHNICAL NOTE 1977-19

6 SEPTEMBER 1977

LEXINGTON   MASSACHUSETTS

FOREWORD

Early in 1972 Lincoln Laboratory made the decision to discontinue the development effort for an Optical Communications link between LES-8 and LES-9. The opportunity to document our early effort never seemed to come. Now, 5 years later, after the launch of LES-8/9, it seems worthwhile to write down some of our thinking on what turned out to be an intriguing problem. Two of the four collaborators are now distantly located and involved in other pressing problems so that it is not possible to write a paper as complete as we would have liked. Here is a slightly edited version of the acquisition analysis we did. Omitted are the interesting but incomplete results for the case of moderate signal-to-noise ratio.

TABLE OF CONTENTS

LIST OF FIGURES

LIST OF TABLES

SPATIAL ACQUISITION IN OPTICAL SPACE COMMUNICATIONS

I. INTRODUCTION

In this note we study the problem of mutual acquisition in space of the direction of pointing of two optical communication transceivers.

In 1970 we undertook the development of an optical communication transceiver for possible application to a satellite-to-satellite link. The transceivers were to establish a two-way communication link at distances of over 40,000 kilometers and data rates of about 10 to 100 kilobits per second. The transmitter employed injection-laser diodes whose optical energy was focused to a transmit beam of about 400 microradian x 100 microradian. We were therefore led to study the problem of mutual acquisition in space of the transmit beams of the two transceivers.

The problem of spatial acquisition of optical beams is common to all optical communication systems,[1,2,3] in which very high antenna gains can be used to achieve good performance with low transmitted energy per bit. Typically the beams which are employed in the communication mode are of the order of 1 to 100 microradians wide. In order to establish communications the transmitter on one satellite must illuminate the other satellite with its transmit beam. This in turn implies a measurement of the angle-of-arrival of optical energy by the receivers in order to allow the transmitters to point in the correct direction. Before the communication link is established there is an initial uncertainty in pointing, which for our satellite system was 17.5 milliradians (1 degree). This uncertainty has several components, the first of which is the uncertainty in the orbital position of the two satellites,

1

which at any given time must be determined from the ground and relayed to the satellite. A second component is contributed by inaccuracies in the attitude control system which maintains the satellite platform in a nominal orientation and counteracts solar torques and other disturbances. Finally, the relative alignment of the transceiver to the platform is uncertain because of calibration errors and of thermoelastic deformations in orbit.

The possible schemes of spatial acquisition of beams can be divided in two general classes. In the first, the transmit beams are maintained in tight collimation during acquisition (order of 1 to 100 microradians) and scanned over a solid angle equal to the uncertainty in the mutual directions of the two satellites A and B. For each position of A's transmit beam the receiver on B performs a search of its angular field-of-view to determine whether it is receiving a legitimate signal or noise only. When a signal is detected by B, the transmit beam of satellite B is immediately aimed in the direction from which energy was received, and the communication link is established as soon as satellite A also detects and acknowledges. An alternative method of ensuring that each satellite sees the transmit beam of the other is to defocus the transmit beams during acquisition.

If the solid angle of the transmit beam equals the solid angle of uncertainty, then with very high probability the receiver on the other satellite is illuminated. Under these conditions, however, the signal energy received by each satellite in the acquisition phase is decreased with respect to that received in the communication mode, in direct proportion to the increase in solid angle occupied by the transmit beam.

This note deals with the determination of the angle-of-arrival of signal energy, a problem which is common to both classes of optical acquisition schemes referred to above. The receiver which we consider is assumed to have a single receive channel, which responds to signals arriving from one direction over one specified field-of-view. A receiver having a large enough number of parallel channels (e.g., a vidicon tube) can in principle make the acquisition process trivial. In practice, however, present devices of this type suffer from high internal noise or do not have a sufficient number of parallel channels (10^6 to 10^8 are needed for some applications). For the above reasons this note describes efficient search procedures of the field-of-view of uncertainty. The term efficient is used in the sense that the time for completion of the acquisition maneuver is minimized with the qualification that we will be referring sometimes to minimum average time and at other times to minimum worst-case acquisition time.

A design for searching the receiver field-of-view utilizes an image-dissector photomultiplier receiver scanned with very fine resolution over a photosensitive surface placed at the focal plane of the receiver. The resolution element ϕ_r is scanned over the field-of-view perhaps using a spiral raster or a television-like linear raster. At each position of the receiver resolution element a decision must be made as to whether there is signal and noise present, or noise only. If we assume, as in our example, a field-of-view of 17.5 milliradian and a resolution of 17.5 microradian, it follows that $M=10^6$ possible positions must be searched for the presence of signals.

Our work started with the simple observation that it must be possible to specify the angular direction of the received signal by means of $\log_2 M$ binary decisions. This corresponds in a physical sense to dividing the field-of-view of uncertainty in two parts and deciding which of the two contains the signal, and then continuing with successive divisions by 2 of the decreasing uncertainty region. However, for our case of $M=10^6$ the receiver must have 20 different fields of view.

For this reason our observation seemed to have purely theoretical value until it was noted that the "binary search" described above would be approximated quite efficiently by "n-ary search": the initial field-of-view is divided in n parts, the decision as to which contains the signal is made, and the new region of uncertainty is again divided in n parts, and so on. For $M=10^6$, $n=2^5=32$, only four distinct fields-of-view are necessary (since the logarithm to base 32 of 10^6 equals approximately 4).

It was also found that it was possible to build an image-dissector photo-multiplier tube which had multiple fields-of-view up to a practical value of four. A prototype tube was built according to our specifications by IT&T.

The binary search decreases substantially the number of decisions to be made. However, the question at hand is that of finding a minimum acquisition time, considering system noise and other constraints.

Logarithmic or binary search methods are used in list searching by computer,[4] in frame synchronization schemes for digital communications, and in analog-to-digital converter design. The idea is also reminiscent of the use of zoom telephoto lenses in TV or film making. In addition, the concepts

are similar to those in measuring the information in a signal.[5]

The body of this report is divided into four parts. In Part II we study the case in which quantum noise dominates over background and detector noise, which can be analyzed in closed form. We find that in addition to the discrete logarithmic search procedures in which the field-of-view is divided into integer fractions there also exist minimum-time continuous scan procedures which are of conceptual interest although not readily implemented. In Part III we study the case of low signal-to-noise ratio, in which background or detector noise dominate. For this case we find that the logarithmic search procedure and the conventional raster-scan search are essentially equivalent from the point of view of search time. In the final part of the report we give some examples referring specifically to our design for the prototype communication system proposed for a satellite optical communication link and we summarize our results.

II. OPTICAL ACQUISITION IN THE HIGH SIGNAL-TO-NOISE-RATIO (QUANTUM-NOISE-LIMITED) CASE

A. Discrete Scan Algorithms

Consider an ideal optical system which maps a field-of-view into a bounded (plane) surface A_o. Let the signal light energy originate from a very distant point source. The signal light collected by the aperture is focused at a point of A_o which uniquely defines the direction (or angle-of-arrival) of signal energy (Fig. 1). Thus, we shall refer to the field-of-view and to the area A_o interchangeably.

The problem to be solved is estimating the angle-of-arrival of signal energy, or equivalently estimating the coordinates of the point on which the received energy is focused. Let A_o be a photosensitive surface which generates electrical charges (e.g., photoelectrons) at a rate proportional to the incident light power. The surface A_o can be searched electronically by means of an image-dissector tube, which is conceptually similar to a television camera. A search area A_1, (Fig. 1) (called the "instantaneous field-of-view"), can be positioned over the area A_o (the "acquisition field-of-view"). This means that the detector is sensitive, at any given time, only to light which impinges on the search area A_1. Traditionally, the surface A_o has been scanned by A_1 in a fixed raster (for example, linear or spiral). For each position of the search area A_1 the decision "Is signal-plus-noise or noise-only present in A_1?" is made. The search stops when the signal is detected. This is the end of acquisition, and the detector system then switches to a tracking mode. Algorithms of this type, in which the search area moves discontinuously, are called "discrete scan" algorithms.

6

PARALLEL LIGHT RAYS
FROM DISTANT SOURCE

IMAGE OF SOURCE

INITIAL ACQUISITION
FIELD-OF-VIEW
(AFOV) ON FACE OF PMT

INSTANTANEOUS SEARCH
FIELD-OF-VIEW
(IFOV)
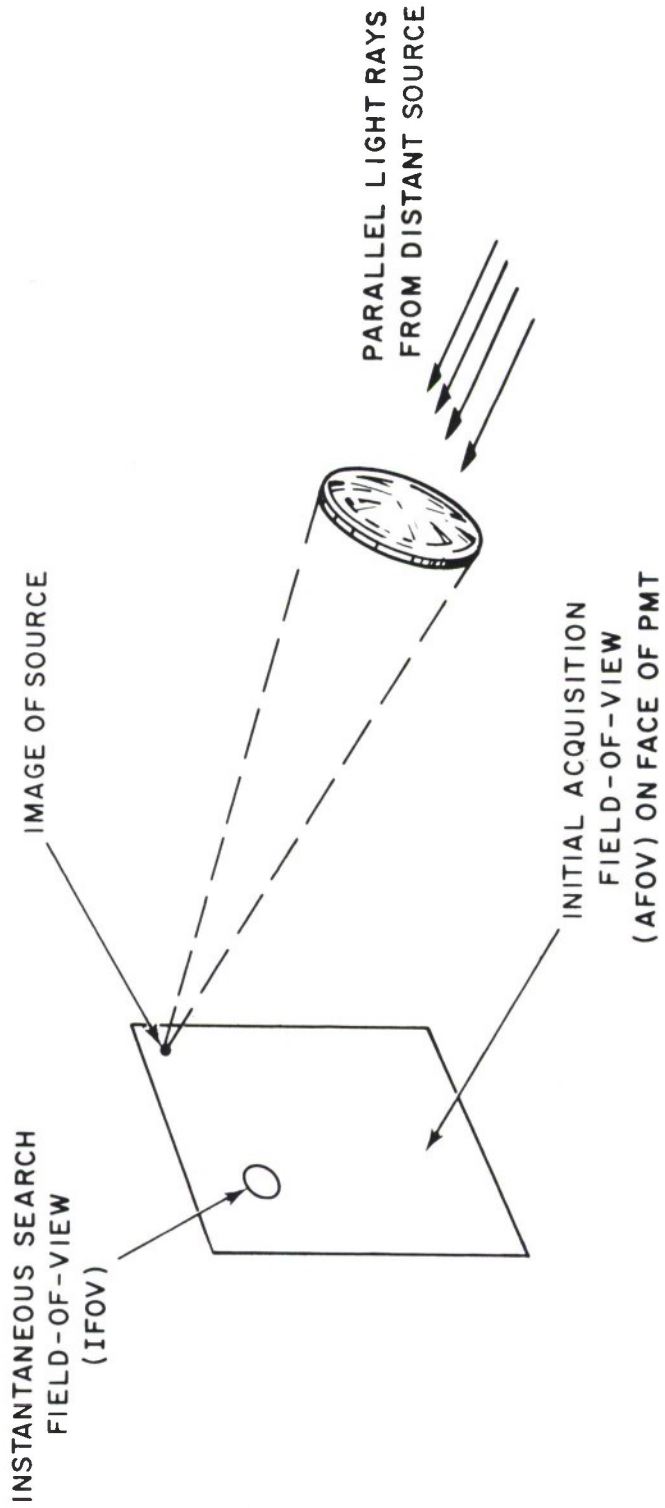
Fig. 1. Image Plane Geometry.

The question then is which algorithm minimizes the time necessary to estimate the angle-of-arrival within the initial field-of-view (FOV) of uncertainty A_o to a final uncertainty, or resolution, A_f.

In this section we assume that the only noise present is due to fluctuations in the time of arrival of photoelectric charges generated by light impinging on the detector surface (quantum noise). The signal obeys Poisson statistics, with rate parameter λ proportional to the power in the signal.

Consider, for example, a simple raster search of the acquisition FOV A_o with a search FOV A_1 equal to the final uncertainty A_f. The basic procedure is to observe each FOV A_f for an "integration time" T, chosen to yield a sufficiently low miss probability $P_m = e^{-\lambda T}$.

The maximum acquisition time T_a is then

$$T_a(\text{raster}) = \frac{A_o}{A_f} T = MT \tag{1}$$

since the integration time is the same for all positions of the search FOV. We have defined $M = \frac{A_o}{A_f}$, as the total number of non-overlapping resolution elements to be searched.

As a second example, consider searching A_o with an intermediate FOV $A_1 > A_f$. There are at most A_o/A_1 decisions to be made to determine which FOV of dimension A_1 contains the signal. One then searches A_1 with a search FOV $A_2 = A_f$. (For simplicity we assume at this point that the ratios A_o/A_1 and A_1/A_f are integers.) The maximum acquisition time is then

8

$$T_a(\text{two FOVs}) = \frac{A_o}{A_1} T + \frac{A_1}{A_f} T$$

If we arbitrarily let $A_1 = (A_o A_f)^{1/2}$, then

$$T_a(\text{two FOVs}) = 2M^{1/2}T$$

If $M = 10^6$, then $2M^{1/2} = 2 \times 10^3$, and the maximum acquisition time has decreased by a factor of 500 with the use of the intermediate FOV A_1. We therefore consider algorithms which use several intermediate FOVs.

Two somewhat different search algorithms which make use of multiple FOVs should be considered. In the first algorithm all search FOVs are examined for the presence of signal before switching to a smaller FOV. In the second algorithm at most all but one of the search FOVs are examined, since it is assumed that, if the search has been unsuccessful in all but one case, the signal is in the last search area. The two classes of algorithms are here called "with check" and "without check."

Consider a sequence of FOVs, $A_o > A_i > A_n$ and define $\alpha_i \equiv A_{i-1}/A_i$. The last FOV must be $A_n = A_f$ to ensure that the final angular uncertainty is achieved. If the α_i's are integers, then

$$\prod_{i=1}^{n} \alpha_i = M \tag{2}$$

---

* FOVs are measured in steradian.

and the acquisition times to be minimized are

$$T_a(\text{with check}) = T \sum_{i=1}^{n} \alpha_i \qquad (3)$$

and

$$T_a(\text{without check}) = T \sum_{i=1}^{n} (\alpha_i - 1) \qquad (4)$$

Let us now consider the more general case in which the α_i's and n are real numbers (not necessarily integers). We shall see later that the case of non-integer α_i's has an interesting physical interpretation.

The minimization is joint over n and the set of values $\{\alpha_i\} \equiv \alpha_1, \alpha_2, \ldots$ α_n. We use a Lagrange-multiplier technique to reduce the problem to a form which can be solved by differentiation.

Defining a function

$$\alpha(t) = \alpha_i \text{ for } (i-1) \le t < i \quad i = \text{integer}$$

we must minimize (considering the <u>algorithm with check</u>)

$$T \sum_{i=1}^{n} \alpha_i = T \int_{0}^{n} \alpha(t) \, dt. \qquad (5)$$

Since

$$\prod_{i=1}^{n} \alpha_i = \exp \left\{ \int_0^n \ln[\alpha(t)]dt \right\}, \tag{6}$$

the constraint equation on (2) can be written[*]

$$\exp \int_0^n \ln[\alpha(t)]dt = M. \tag{7}$$

Using the Lagrange multiplier γ, we must minimize

$$F \equiv T \int_0^n \alpha(t)dt + \gamma \exp \left\{ \int_0^n \ln[\alpha(t)]dt \right\} - M \tag{8}$$

with respect to the α_i's, n and γ.

The following three equations result:

$$\frac{\partial F}{\partial \alpha_i} = T + \frac{\gamma}{\alpha_i} \exp \left\{ \int_0^n \ln[\alpha(t)]dt \right\} = 0 \tag{9}$$

$$\frac{\partial F}{\partial \gamma} = \exp \left\{ \int_0^n \ln[\alpha(t)]dt \right\} - M = 0 \tag{10}$$

$$\frac{\partial F}{\partial n} = T\alpha(n) + \gamma \ln[\alpha(n)] \exp \left\{ \int_0^n \ln[\alpha(t)]dt \right\} = 0 \tag{11}$$

Using (10) in (9),

$$\alpha_i = -\frac{\gamma M}{T} \equiv \alpha. \tag{12}$$

---

[*] Note that since n is real, the constraint equation can always be written as an equality.

It is an important result that all α_i's are equal and therefore $\alpha(t)$ is constant. Using this result and (10) in (11), we obtain

$$\ln\alpha = 1 \tag{13}$$

and therefore the optimum solution is, using (10) and (7),

$$\alpha_{opt} = e = 2.718...$$

$$n_{opt} = \ln M$$

The minimum acquisition time is

$$T_{a,min} = e \; n_{opt} T = e(\ln M)T \tag{14}$$

Comparing this with (1), we see that the acquisition time, using the optimum search, is reduced by a factor $(e \ln M)/M \ll 1$ for large M.

Slight modifications to these results are necessary, if we constrain α and n to be integers. The fact that all α_i's must be equal still holds, as can be seen directly by rewriting (3) as

$$T_a = T \sum_{i=1}^{n} \frac{A_{i-1}}{A_i} \tag{15}$$

12

and setting $\partial T_a / \partial A_j = 0$.

From (2) and (3) the problem reduces to

$$\alpha n = \min$$
$$\alpha^n \geq M \tag{16}$$
$$n, \alpha \text{ integers}$$

where the constraint must now be written as an inequality.

The solution to this problem is not independent of the value of M. For small M, either $\alpha=2$ or $\alpha=3$ is best. For example, if M=100, then $n_{(\alpha=2)}=7$ and $n_{(\alpha=3)}=5$, and αn is minimized for $\alpha=2$. If M=80, then $n_{(\alpha=2)}=7$ and $n_{(\alpha=3)}=4$, and $\alpha=3$ is the preferred solution.

To find the optimum for large M, we can write from $\alpha^n \geq M$

$$\log_\alpha M \leq n(\alpha) \leq 1 + \log_\alpha M \tag{17}$$

Multiplying by $\alpha/\ln M$ and developing $\log_\alpha M$,

$$\frac{\alpha}{\ln \alpha} \leq \frac{\alpha n(\alpha)}{\ln M} \leq \frac{\alpha}{\ln M} + \frac{\alpha}{\ln \alpha} \tag{18}$$

and the upper bound is seen to approach the lower bound for large M. Since the minimum of $\alpha/\ln \alpha$ occurs for $\alpha=3$ for α integer, this value also minimizes $\alpha n(\alpha)$ for large M.

In practice there is not a great difference in performance between $\alpha=2$,

13

$\alpha=e$ and $\alpha=3$. The choice must be determined by considerations of implementation. It will be seen in the following that the solution $\alpha=e$ has an interesting physical interpretation.

Considering now the algorithm without check, Eq. (3) must now be replaced by Eq. (4)

$$T_a(\text{without check}) = T \sum_{i=1}^{n} (\alpha_i - 1) \qquad (4)$$

while Eq. (2) stands. The same procedure as above leads to the condition

$$\frac{\alpha-1}{\ln\alpha} = \alpha \qquad (19)$$

instead of (13). This equation has a solution $\alpha=1$ which is not acceptable, since α must exceed unity. Since the absolute minimum for the acquisition time occurs at $\alpha=1$, and there are no relative minima, the acquisition time is an increasing function of α. Therefore, the best integer value for α is 2.

The results are summarized in Table I.

TABLE I

RATIOS OF SUCCESSIVE FIELDS-OF-VIEW FOR OPTIMUM DISCRETE SCANS

Type of Search	α Optimum Ratio of Successive Fields-of-View	
	General Algorithm	Integer
With Check	$e = 2.718...$	for small M: 2 or 3 (depending on M) for large M: 3
Without Check	2	2

If one interprets the i-th stage of search as a stepwise fitting of A_i into A_{i-1} precisely α times, a certain inefficiency results unless α is integer. When α is integer, the physical realization of the optimum search involves the use of detection systems capable of adjusting their field-of-view in steps successively decreasing by α. Since n $\simeq$ $\log_\alpha$M is a large number for practical values of M, the receiver is required to have very many FOVs. However, we shall see in Section IV that optimum performance can be approximated well by using only a few receiver fields-of-view, and that these "suboptimum receivers" are physically realizable and have considerable practical interest.

B.   Continuous Scan Realization and Analysis of the Average
     Acquisition Time

The optimum value of the ratio $\alpha = A_{i-1}/A_i$ of successive fields-of-view is e=2.718... for the general algorithm with check, as we have seen. It is interesting to note that this general algorithm can be realized, at least in principle, by using two continuous scan techniques, which are described in the following.

The first scheme consists of a shutter covering a half-plane, which is moved at a variable velocity v_i across the field-of-view. The second approach uses a mask composed of alternating open and obscured segments, which is passed at high speed across the FOV. In both cases, we shall consider the quantum-noise-limited case and simplify the analysis by considering only a one-dimensional search, although the techniques generalize readily to two dimensions.

The mechanization of the first scheme is simple, and its analysis is intuitively satisfying. However, the analysis takes no account of edge

15

effects occurring when the shutter moves beyond the boundary of the field-of-view. In this respect the analysis is approximate; worse, the nature of the approximation is difficult to analyze. The second approach, while more difficult to implement, leads to a correct answer in closed form, without edge effects.

Figure 2 illustrates the variable-velocity configuration during the i-th step of the scan. At some instant of time, the moving shutter will disclose the source, and τ_i seconds thereafter a photon will arrive. Since photon arrivals obey Poisson statistics, the quantity τ_i is an exponentially-distributed random variable with probability density function

$$p_{\tau_i}(\rho_i) = \lambda e^{-\lambda \rho_i}, \tag{20}$$

in which λ is the average arrival rate of the photons. Consequently, the distance $u_i = v_i \tau_i$ travelled by the shutter after disclosure of the source is also an exponential random variable, with

$$p_{u_i}(\phi_i) = \frac{\lambda}{v_i} e^{-\frac{\lambda}{v_i} \phi_i}. \tag{21}$$

Equation (21) describes the state of our current knowledge of the position of the source, after the i-th step of the scan.

Suppose the shutter now flips over from right to left, so that the left half-plane is obscured (including the source, which is u_i meters to the left of the shutter boundary). Let the shutter instantaneously begin moving to

16
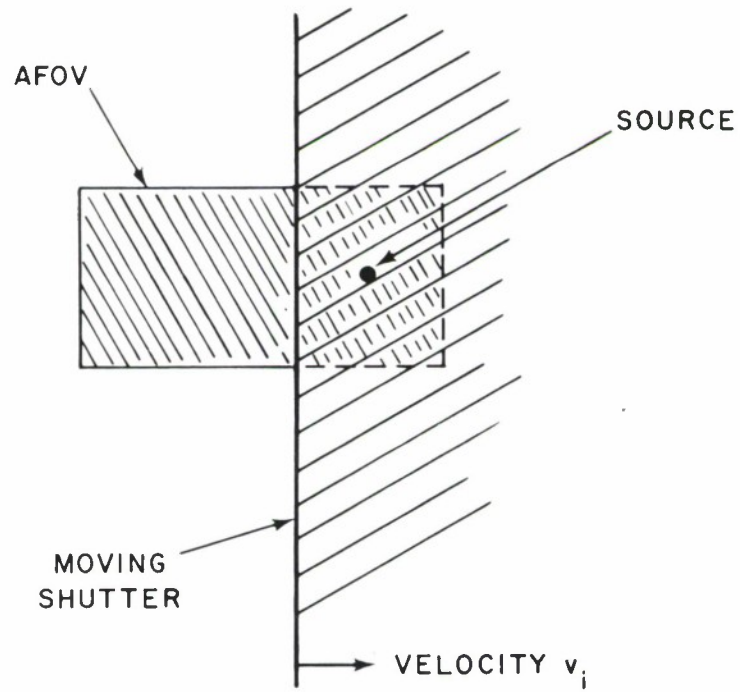
Fig. 2. Variable-velocity Continuous Scan Configuration.

17

the left at a (slower) velocity v_{i+1} meters per second. Exactly θ_{i+1} second later, the source will again be disclosed, where $\theta_{i+1} = \dfrac{u_i}{v_{i+1}}$ is an exponentially-distributed random variable with mean value $v_i/(\lambda v_{i+1})$. τ_{i+1} seconds after that point, the first photon will arrive, where τ_{i+1} obeys Eq. (20). In general, the time duration of the i-th step of the scan is

$$T_i = \theta_i + \tau_i. \tag{22}$$

The scan is complete when, after n steps, the distance u_n from the shutter boundary back to the source is known to within some desired resolution A_o/M, where A_o was the initial FOV. Clearly, this implies that v_n must be of the order of v_o/M. Thus

$$T_s = T_o + \sum_{i=1}^{n} (\theta_i + \tau_i), \tag{23}$$

in which T_o, the time to arrival of the first photon in the first step, depends upon a priori statistics of source location. The average total scan time is

$$\overline{T}_s = \overline{T}_o + \sum_{i=1}^{n} \left(\frac{v_{i-1}}{\lambda v_i} + \frac{1}{\lambda} \right) \tag{24}$$

$$= \overline{T}_o + \sum_{i=1}^{n} \left(\frac{v_{i-1}}{v_i} + 1 \right) \tag{24}$$

18

The minimization of Eq. (24) follows as before. We find that

$$\overline{T}_s = \overline{T}_o + \frac{\alpha \ln M}{\lambda} \,, \tag{25}$$

because of the term +1 under the summation sign in Eq. (24), the optimum value of α for this problem is found to be slightly greater than 3.

The second continuous-scan configuration is shown in Fig. 3. Suppose L_{o1} and L_{c1} are so chosen that their sum equals A_o, the width of the initial FOV. When the first photon reaches the detector, the position of the mask at that instant delineates the source position to within a resolution of L_{o1} meters. Now, let the initial mask be replaced by a finer-grained mask, in which the length L_{c2} of a closed segment plus the length L_{o2} of an open segment equals L_{o1}. (This new mask could be an adjacent ring on a drum of graduated masks, which can be mechanically positioned in sequence between the FOV and the detector.) When the next photon arrives, we shall know which portion L_{o2} contains the source. Repeating this procedure, we shall ultimately use a mask having open portions L_{on} equal in length to the desired final resolution A_o/M.

Let us estimate the optimum number and duty cycle of the masks. If the i-th mask were to rotate continuously at tangential velocity v_i across the tube face, the arrival of photons at the detector would be a segmented Poisson process with alternating "on" and "off" periods lasting

$$\Delta_{oi} = L_{oi}/v_i, \tag{26}$$

19

18-6-18430

SOURCE

AFOV

ROTATING MASK

L_{CI}

L_{OI}

V
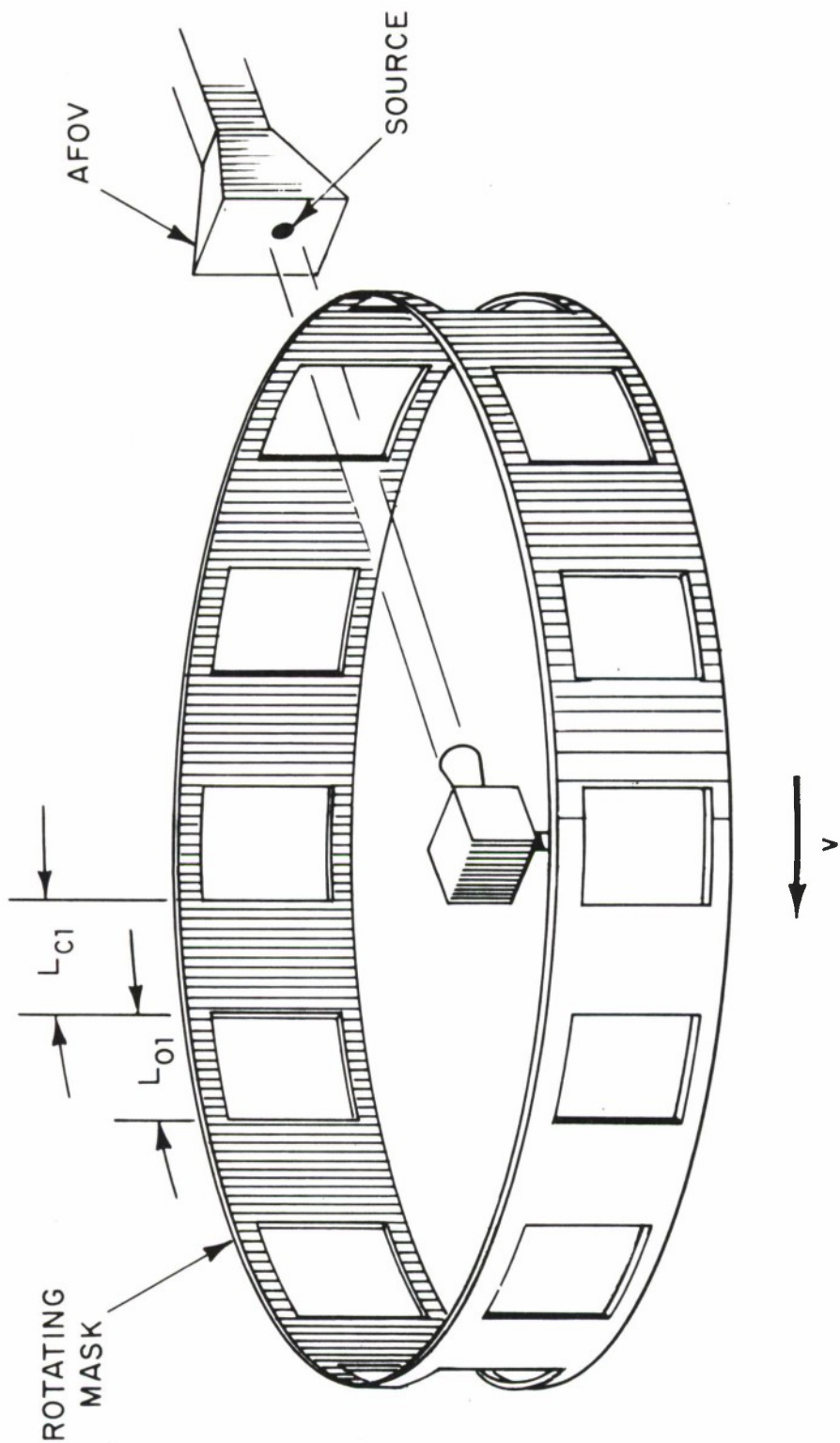
Fig. 3. Abbreviating-mask Continuous Scan Configuration.

20

and

$$\Delta_{ci} = L_{ci}/v_i, \tag{27}$$

seconds, respectively. We shall derive the probability density function $p_\tau(t)$ of the waiting time τ to arrival of the first photon in such a process. To do this, we compute and then differentiate the probability distribution function

$$f_\tau(t) = \text{Pr } \{\tau \leq t\},$$

$$= 1 - \text{Pr } \{\tau > t\}, \tag{28}$$

$$= 1 - \text{Pr } \{\text{zero photons arrive in } t\}.$$

Assuming that the first "on" period Δ_{oi} starts at $t=0$, as in Fig. 4, we have

$$F_\tau(t) = \begin{array}{ll} 1 - e^{-\lambda t} & , \quad 0 < t \leq \Delta_{oi}; \\ 1 - e^{-\lambda \Delta_{oi}} & , \quad \Delta_{oi} < t \leq \Delta_{oi} + \Delta_{oi}; \\ 1 - e^{-\lambda(t-\Delta_{oi})} & , \quad \Delta_{oi} + \Delta_{ci} < t \leq 2\Delta_{oi} + \Delta_{ci}; \\ \qquad \vdots \end{array} \tag{29}$$

whence

$$\rho_\tau(t) = \begin{cases} \lambda e^{-\lambda(t-k\Delta_{oi})}, & k(\Delta_{oi}+\Delta_{ci}) < t \leq [(k+1)\Delta_{oi} + k\Delta_{ci}], k=0,1,2,\ldots \text{ as;} \\ \\ 0, & \text{elsewhere.} \end{cases} \tag{30}$$

The mean value $\bar{\tau}$ is readily computed; we have

$$\bar{\tau} = \int_0^{\infty} t \, p_{\tau}(t) \, dt$$

$$= \sum_{k=0}^{\infty} \int_{k(\Delta_{oi}+\Delta_{ci})}^{(k+1)\Delta_{oi} + k\Delta_{ci}} \lambda t e^{-\lambda(t-k\Delta_{oi})} dt$$

$$= \frac{1}{\lambda}\left[1 + \left(\lambda \, \frac{\lambda\Delta_{oi}}{e^{\lambda\Delta_{oi}}-1} \right)\right] . \tag{31}$$

in which

$$\gamma = \frac{\Delta_{ci}}{\Delta_{oi}} = \frac{L_{ci}}{L_{oi}} . \tag{32}$$

By an equally straightforward (though rather more tedious) calculation, we find that

$$\mathrm{Var}(\tau) = \overline{\tau^2} - \bar{\tau}^2$$

$$= \frac{1}{\lambda^2}\left[1 + \frac{\lambda^2\Delta_{oi}^2 \, e^{-\lambda\Delta_{oi}}}{1 - e^{-\lambda\Delta_{oi}}{}^2}(2\lambda+\lambda^2)\right] \tag{33}$$

Equations (31) and (33) are of particular interest when $\lambda\Delta_{oi} \ll 1$, corresponding to a high tangential velocity. Under this condition we have effectively a simple Poisson process, with rate parameter diminished by the

22

factor $1/(1+\lambda)$; Eqs. (31) and (33) reduce to

$$\bar{\tau} \sim \frac{1}{\lambda} (1 + \gamma) \tag{34}$$

and

$$\text{Var}(\tau) \sim \frac{1}{\lambda^2} (1 + \gamma)^2 \tag{35}$$

We observe that

$$1 + \gamma = \frac{L_{ci} + L_{oi}}{L_{oi}}$$

$$= \frac{L_{o,i-1}}{L_{oi}} \tag{36}$$

the familiar ratio of successive fields-of-view. The mean time duration $\bar{T}_s$ of an entire scan is obtained by summing $\bar{\tau}$ over n successive steps. We have

$$\bar{T}_s = \frac{1}{\lambda} \sum_{i=1}^{n} \frac{L_{o,i-1}}{L_{oi}}$$

$$= \frac{1}{\lambda} \sum_{i=1}^{n} \alpha_i \tag{37}$$

where, by definition, L_{oo} is equal to A_o and $L_{o,n}$ is equal to A_o/M. We may show, as before, that $\bar{T}_s$ is minimized by choosing $n=\ln M$ and $\alpha=e$ for all i, whence

23

$$\overline{T}_s = \frac{e \ln M}{\lambda} \tag{38}$$

Since T_s is the sum ot statistically independent random processes, its variance is the sum of n terms similar to Eq. (35); we find that

$$\text{Std. dev. } (T_s) = \frac{e}{\lambda} \sqrt{\ln M} \tag{39}$$

It is interesting to compare Eq. (38) above for the expected acquisition time, to the maximum acquisition time with check given by Eq. (14):

$$T_{a,max} = e \ln M. \, T \tag{40}$$

We note that the expected acquisition time is obtained simply by re-placing T with $1/\lambda$, the average time between photons.

III. OPTICAL ACQUISITION IN THE LOW SIGNAL-TO-NOISE-RATIO CASE

A. The Detection Statistics

This section is concerned with the signal levels required at the receiver to ensure that desired false-alarm and acquisition probabilities are achieved during an optical communication system's acquisition phase.

The acquisition procedure considered assumes that the receiver's acquisition field-of-view (AFOV) is scanned with a narrower receiver instantaneous field-of-view (IFOV). It is assumed that the beacon beamwidth is large enough to ensure that the receiver is illuminated; if this is not the case, the acquisition time will be increased because the beacon beam must be scanned until the receiver is illuminated. The beacon may be operating in either a pulsed mode, with pulse width τ_t and repetition rate f_s, or in a CW mode.

If the source is pulsed, the IFOV is held fixed for $1/f_s$ seconds and the detector output during this time is fed to a sliding integrator. The integration limits depend on time t so that a τ_b second integration interval is moved over the $1/f_s$ time period, i.e., the integrator forms $\int_t^t (\cdot) dt$. (The integrator corresponds to the matched filter if $\tau_b = \tau_t$.) The integrator output is compared continuously with a threshold γ_a. If γ_a is exceeded at some time t_1, the IFOV is held fixed and the filter output at time $t_1 + 1/f_s$ is compared with a threshold γ_v to verify the acquisition. If γ_v is exceeded it is assumed that acquisition has occurred and the receiver enters a tracking mode. If γ_a is not exceeded, the IFOV is scanned to the next position. The verification procedure makes it possible to achieve reliable acquisition even though the probability of a false alarm relative to threshold γ_a is relatively large. Indeed the verification procedure could integrate over several signal pulses if necessary.

25

If the source is CW, the IFOV is held fixed for a time τ. The detector output is integrated for this period of time and then compared to a threshold γ_a. If γ_a is exceeded, acquisition is verified by holding the IFOV fixed for τ_v seconds, integrating the detector output for τ_v seconds, and comparing the integrated value with threshold γ_v.

For either a pulsed or CW source if γ_a is not exceeded for a given position of the IFOV, the IFOV is scanned to the next position. If γ_a is not exceeded for any position of the IFOV within the AFOV, the entire procedure repeats itself.

Thus associated with any complete scan of the AFOV there are three possibilities: correct acquisition, false acquisition, and no acquisition. The probabilities of these three events depend, in general, on the number of IFOV's examined before the IFOV that contains the signal and, for pulsed operation, even on the pulse position within the $(1/f_s)$-second time interval associated with the correct IFOV. For analysis purposes the problem can be thought of as a detection problem in which each of

$$M = \left(\frac{\theta_a}{\theta_r}\right)^2 / f_s \tau_b \qquad (41)$$

resolution cells is tested in sequence for the presence of a signal until a signal is detected. (For a CW source assume $\tau_b = 1/f_s$.) Here θ_a is the acquisition field-of-view width and θ_r is the receiver field-of-view width.

If the detection problem is adequately modeled as a decision between two Poisson distributions with parameters $n_s + n_b$ and n_b respectively, an analysis, which is carried out in the next section, establishes the following performance bounds:

$$P_{af} < P_{v_f} \exp\left\{-(n_s + n_b)\left[1 - \frac{\ln\alpha}{\alpha} - \frac{1}{\alpha}\right]\right\} \tag{42a}$$

$$P_{ac} > (1-P_{v_c})\left(1 - \exp\left\{-(n_s + n_b)\left[1 - \frac{\ln\alpha}{\alpha} - \frac{1}{\alpha}\right]\right\}\right)^2 \tag{42b}$$

Here:

$P_{af} \overset{\Delta}{=}$ probability that receiver acquires incorrectly during a scan of AFOV

$P_{ac} \overset{\Delta}{=}$ probability that receiver acquires correctly during a scan of AFOV

$P_{v_f} \overset{\Delta}{=}$ probability that integrator output exceeds γ_v during
confirmation mode when the beacon signal is not present.

$P_{v_c} \overset{\Delta}{=}$ probability that integrator output exceeds γ_v during
confirmation mode when the beacon signal is present

$n_s \overset{\Delta}{=}$ average number of detected signal photons in τ_b-second interval

$n_b \overset{\Delta}{=}$ average number of detected noise photons in τ_b-second interval

$$\alpha \overset{\Delta}{=} \frac{n_s + n_b}{n_s + \ln(M-1)} \ln(1 + n_s/n_b) = \frac{\mu+1}{\mu+r'} \ln(1+\mu) \tag{42c}$$

$$\mu \overset{\Delta}{=} n_s/n_b \tag{42d}$$

$$r' \overset{\Delta}{=} \frac{\ln(M-1)}{n_b} \tag{42e}$$

Here α must satisfy $\alpha \geq 1$ for the bound to be valid. Note that the performance depends on n_s, μ, and r', which are respectively the number of signal counts, the signal to noise count ratio, and an information rate in nepers per noise count. This is true because n_s+n_b can be written as $n_s(1+1/\mu)$, and for any verification threshold, γ_v, P_{vf} and P_{vc} also depend on these parameters.

27

From the bounds of Eq. 42 it is clear that, in the absence of the verification step, the acquisition performance depends on the exponent

$$n_s(1+1/\mu)[1-\ln \alpha/\alpha - 1/\alpha] \tag{43}$$

For example, if this exponent is 4.6, then

$$P_{af} \leq 10^{-2} \quad \text{and} \quad P_{ac} \geq 0.98 \ (P_{vf} = 1 \quad \text{and} \quad P_{vc} = 0) \quad .$$

In the following the value of this exponent will be denoted as C. We wish to solve for the value of n_s required to make the exponent equal a desired C value given the values of n_b and M. Note that n_b and M are determined by the choice of the various receiver parameters and the level of the background radiation and detector dark current.

For $\mu \ll 1$, the value of n_s required to achieve a desired value of C is given by

$$n_s = \sqrt{2n_b} \ [\sqrt{C} + \sqrt{C+\ln(M-1)}] \tag{44}$$

This result, which is valid for $\mu < 0.3$ and $r \overset{\Delta}{=} r'/\mu < \mu/2$, is obtained by noting that the exponent can be approximated as

$$\frac{1}{8} n_s \mu \frac{[1-2r/\mu]^2}{1+r} \approx \frac{1}{8} n_s \mu[1-2r/\mu]^2 \tag{45}$$

for μ and r (or r') in this range. The parameter r is an information rate in nepers per signal count. For other values of μ it is difficult to obtain an analytical result although we have obtained graphical solutions which are omitted here.

28

B. Acquisition Probabilities

For any complete scan of the AFOV there are three possible outcomes: correct acquisition, false acquisition, and no acquisition. The probabilities of these three events are the quantities of interest. For analysis purposes the problem can be thought of as a detection problem in which each of M resolution cells is tested in sequence for the presence of a signal until a signal is detected or the scan is finished.

Assume that the beacon occupies the ith of the M time/solid-angle resolution cells. Then the relevant probabilities are

$$P_{na} = (1-P_{v_f})[1-(1-P_f)^i(1-P_m)] + P_m\, P_{v_f}\,(1-P_f)^{M-1} \tag{46a}$$

$$+ (1-P_f)^i(1-P_m)\, P_{v_m}$$

$$P_{ac} = (1-P_f)^i(1-P_m)(1-P_{v_m}) \tag{46b}$$

$$P_{af} = P_{v_f}[1-(1-P_f)^i] + P_m\, P_{v_f}[(1-P_f)^i - (1-P_f)^{M-1}] \tag{46c}$$

where

$P_{na} \triangleq$ probability of no acquisition during scan of AFOV

$P_{ac} \triangleq$ probability of correct acquisition during scan of AFOV

$P_{af} \triangleq$ probability of false acquisition during scan of AFOV

$P_f \triangleq$ probability of exceeding γ_a when beacon signal is not present

$P_m \triangleq$ probability of not exceeding γ_a when beacon signal is present

$P_{v_f} \triangleq$ probability of exceeding γ_v when beacon signal is not present

29

$P_{v_m} \triangleq$ probability of not exceeding γ_v when beacon signal is present

and γ_a and γ_v are respectively the acquisition and verification thresholds. If all values of i are equally probable the average values of the probabilities are

$$\overline{P}_{na} = (1-P_{v_f})\left\{1 - \left[\frac{1-(1-P_f)^M}{MP_f}\right](1-P_M)\right\} + P_m P_{v_f}(1-P_f)^{M-1}$$
$$+ (1-P_m)P_{v_m}\left[\frac{1-(1-P_f)^M}{MP_f}\right] \tag{47a}$$

$$\overline{P}_{ac} = (1-P_{v_m})(1-P_m)\left[\frac{1-(1-P_f)^M}{MP_f}\right] \tag{47b}$$

$$\overline{P}_{af} = P_{v_f}\left(1 - \left[\frac{1-(1-P_f)^M}{MP_f}\right]\right) + P_m P_{v_f}\left[\frac{1-(1-P_f)^M}{MP_f} - (1-P_f)^{M-1}\right] \tag{47c}$$

The choice of i = M-1 is a worst case in the sense that P_{af} is maximized and P_{ac} is minimized. These values are

$$\left(P_{af}\right)_{max} = P_{v_f}[1-(1-P_f)^{M-1}] \tag{48a}$$

$$\left(P_{ac}\right)_{min} = (1-P_m)(1-P_{v_c})(1-P_f)^{M-1} \tag{48b}$$

Under the assumption that it is adequate to model the detection problem of interest as the discrimination between two Poisson processes, the false-alarm and miss probabilities P_f and P_m can be bounded. These bounds are (see Ref. 6).

30

$$P_m < e^{-(n_s+n_b)+\gamma_a+\gamma_a \ln[(n_s+n_b)/\gamma_a]} \tag{49a}$$

$$P_f < e^{-n_b+\gamma_a-\gamma_a \ln[\gamma_a/(n_b)]} \tag{49b}$$

where n_s and n_b are the average number of detected signal and noise photons in the detection interval. If γ_a is set to minimize the probability of a wrong decision on any one of the M decisions

$$\gamma_a = \frac{n_s+\ln(M-1)}{\ln(1+\mu)} \quad . \tag{49c}$$

where it is assumed that the probability that a signal is present is 1/M. This leads to the bounds

$$P_m < e^{-(n_s+n_b)[1-\ln\alpha/\alpha-1/\alpha]} \tag{50a}$$

$$P_f < \frac{1}{M-1} e^{-(n_s+n_b)[1-\ln\alpha/\alpha-1/\alpha]} \tag{50b}$$

where

$$\alpha = \frac{n_s+n_b}{n_s+\ln(M-1)} \ln(1+n_s/n_b) \tag{50c}$$

The bounds are only valid for $\alpha > 1$.

For convenience in discussing these bounds we introduce the parameters

$$\mu \overset{\Delta}{=} \frac{n_s}{n_b} \tag{51a}$$

$$r = \frac{\ln(M-1)}{n_s} \tag{51b}$$

and

$$r' = \frac{\ln(M-1)}{n_b} \tag{51c}$$

31

Here μ is a signal-to-noise ratio, r is essentially an information rate in nepers per signal photon, and r´ is an information rate in nepers per noise photon.

In Ref. 6 the bounds of Equation 50 are analyzed for the case where $r \approx 0$. In this case the exponent behavior depends only on μ; for $\mu < 0.3$ the exponent in Equation 50 is approximately $1/8 \, n_s \mu$, for $\mu = 1$ the exponent is $0.1 \, n_s$, and for $\mu \to \infty$ the exponent is n_s.

In the more general case where r is not negligible the behavior of the bound exponent is more complex. For $\mu < 0.3$ and $\mu > 2r$ the exponent is

$$\text{Exp} \approx 1/8 \, n_s \, \mu \, \frac{[1-2r/\mu]^2}{1+r} \qquad , \qquad (52a)$$

for $\mu = 1$ and $r < 2 \ln 2 - 1$ the exponent is

$$\text{Exp} = 2 \, n_s \left[\frac{\dfrac{2 \ln 2}{1+r} - \left[\ln \dfrac{2 \ln 2}{1+r}\right] - 1}{\dfrac{2 \ln 2}{1+r}} \right] , \qquad (52b)$$

and for $\mu \gg 1$ and $1+r < \ln(1+\mu)$

$$\text{Exp} = n_s \left\{ \frac{\dfrac{\ln(1+\mu)}{1+r} - \ln \left[\dfrac{\ln(1+\mu)}{1+r}\right] - 1}{\dfrac{\ln(1+\mu)}{1+r}} \right\} . \qquad (52c)$$

In terms of the results of Equation 48 and the bounds of Equation 50,

$$P_{a_f} < P_{v_f} \, e^{-(n_s+n_b)[1-\ln\alpha/\alpha-1/\alpha]} \qquad (53a)$$

$$P_{a_c} > (1-P_{v_c}) \left(1 - e^{-(n_s+n_b)[1-\ln\alpha/\alpha-1/\alpha]} \right)^2 \qquad (53b)$$

32

Thus the acquisition performance can be evaluated in terms of n_s, n_b and M (for any verification threshold γ_v, P_{v_f} and P_{v_c} will depend on n_s and n_b). Alternatively, the performance depends on n_s, μ, and r'.

C. Acquisition Strategies

In this section we compare the linear scan and the logarithmic (binary) scan under the assumption of very low signal-to-noise ratio. In the previous sections it was shown that the number of signal counts, n_s, required to achieve a given acquisition performance was related to an exponent C that was given by

$$n_s = \sqrt{2n_b} \, K_o \tag{54}$$

where

$$K_o = \sqrt{C} + \sqrt{C + \ln(M-1)}$$

Let the dwell time be T, the signal photon rate be λ_s, and the noise photon rate be λ_n. Then we can solve for the dwell time and obtain:

$$T = \frac{2\lambda_n}{\lambda_s^2} K_o^2 \quad . \tag{55}$$

This result is very significant because it emphasizes the importance of signal strength; doubling the signal decreases the search time by a factor of 4. Taking advantage of this fact for mutual acquisition of two transceivers is discussed later.

The acquisition time for a linear scan is now computed. Let λn be the noise photon rate for the acquisition (full field-of-view) (AFOV). Let M be the number of instantaneous field-of-views (IFOV) to be searched. Then the search time for each position is

$$T_i = \frac{2\lambda_n K_o^2}{M\lambda_s^2} \tag{56}$$

The total search time T is

$$T = \sum_1^M T_i = MT_i = \frac{2\lambda_n K_o^2}{\lambda_s^2} \tag{57}$$

The acquisition time for a binary scan is now computed. The ith instantaneous field-of-view $IFOV_i$ has a noise photon rate

$$\lambda_{ni} = \lambda_n \times 2^{-i} \tag{58}$$

The total search time is

$$T = \sum_{i=1}^I \frac{2\lambda_n K_o^2}{\lambda_s^2} 2^{-i} \tag{59}$$

$$\approx \frac{2\lambda_n K_o^2}{\lambda_o^2} \qquad \text{for large I} \tag{60}$$

$$I = \log_2 \left[\frac{AFOV}{IFOV}\right]$$

Thus the total search time is approximately the same for a linear scan or a binary scan. This conclusion rests heavily on the original assumption that the signal-to-noise ratio is always small, even for the smallest instantaneous field-of-view, namely

$$\frac{\lambda_s M}{\lambda_n} \ll 1 \quad .$$

34

IV. APPLICATIONS

   A. Satellite-to-Satellite Optical Link

   In this section we apply the results obtained above to the design of a specific optical communication system.

   A first application is an optical two-way link between two satellites in coplanar, synchronous circular orbits. The parameters assumed for the design are summarized in Table II. Ten GaAs diode lasers are pulsed sequentially at a repetition rate of 3,125 pulses/sec (or an overall rate of 31,250 pulses/sec), with a peak power of 4 watts and energy per pulse of 10^{-7} joule. Pulse position modulation permits transmission at a rate of 125 kbit/sec. The rate achievable is limited by the characteristics of the laser source available.

   Since the acquisition field of view is 17.45 millirad, while the required resolution is 17.45 microrad, there are 10^{6} possible source locations within the field of view. As seen above, this would imply that the optimum search strategy (for the quantum-noise-limited case) would require $20 \log_{2} 10^{6} \simeq 14$ distinct fields-of-view. This large number of FOVs is impractical, and therefore we turn our attention to suboptimal systems, which use only a few distinct fields-of-view.

   In the quantum-noise-limited case the scan time is bounded by

$$T_{a} \leq Tn\alpha \leq T(1+\log_{\alpha}M) \quad \alpha \tag{61}$$

The results are summarized in Table III, which shows both the absolute time and the time relative to the optimum.

   One sees that there is very little difference between $\alpha = 2$, $\alpha = e$ and $\alpha = 3$. More importantly, one sees that with 4 FOVs (which corresponds to

35

$\alpha = 32$), the acquisition time is only 3.33 times worse than optimum. On the other hand, a full linear scan requires an acquisition time 26,000 times longer than optimum and quite long in the absolute (2.8 hours). Thus it is seen that in the quantum-noise-limited situation a suboptimum receiver with four fields-of-view closely approximates the optimum acquisition receiver with 14 FOVs.

One possible realization of a receiver with four fields-of-view is shown in Fig. 4. It is a special image-dissector tube, whose aperture plate has four apertures backed up by four separate dynode chains. The field-of-view is selected by electronic switching between the four dynode chains. Table III gives the performance parameters for this four-aperture tube.

If the direction of the other satellite is known at a given time to an accuracy A_i, there is an advantage to using a transmit beam of angular extent A_i, since the energy received by the other satellite is increased in this manner. Therefore during acquisition three different transmit beamwidths and five different receiver fields-of-view are used. The widest beamwidth and field-of-view (17.45 mrad or 1°) are approximately the same and are large enough to guarantee essentially that the prior pointing accuracy places the transmit beam of each satellite in the receiving field-of-view of the other. The defocused transmit beams are obtained by inserting extra lenses in the transmitter optical system. The widest receiver field-of-view is determined by the receiver. The other four receiver fields-of-view are achieved using different apertures in the image-dissector tube as described above.

APERTURES

FOCUSING AND
DEFLECTION COILS

2.5-cm-DIAMETER
PHOTOCATHODE

- 6 - 18431

ELECTRICAL
SIGNAL OUT

ONE OF FOUR
ELECTRON-MULTIPLIER
STRUCTURES

APERTURES

PHOTOELECTRONS

OPTICAL SIGNAL IN
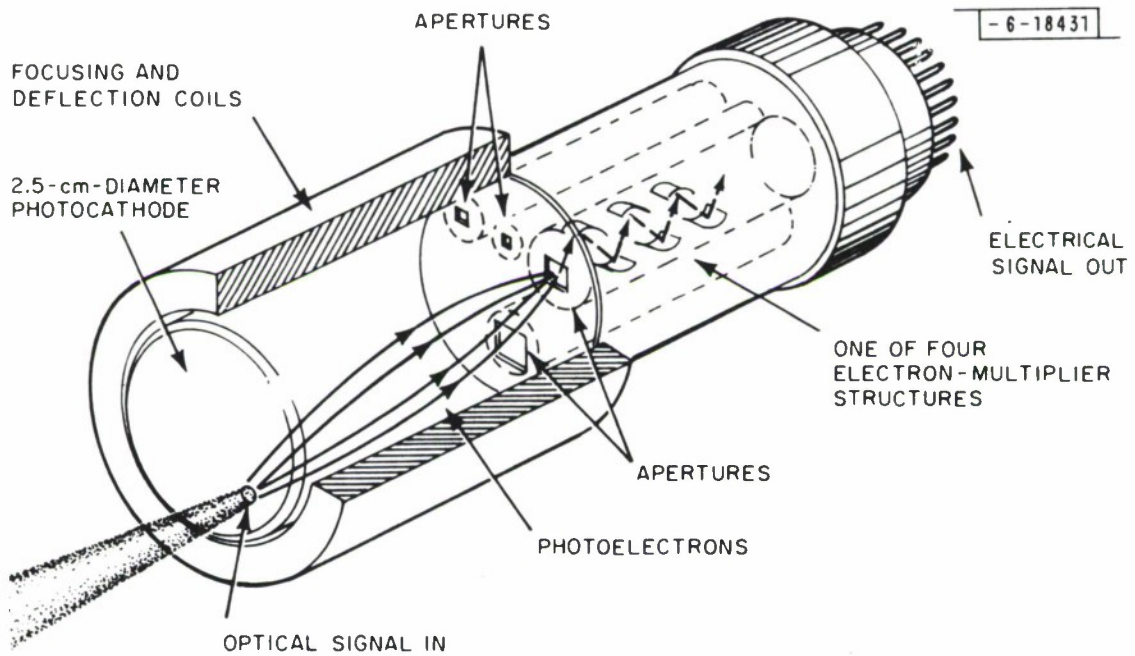
CHARACTERISTICS

QUANTUM EFF: 3% AT 0.85 μm
GAIN: 10^6
BANDWIDTH: 40 MHz
RESOLUTION: 1000 SPOTS / DIAMETER
(smallest aperture)

Fig. 4. Four-aperture Image Dissector Tube.

The first step of the acquisition procedure is to scan the full 17.45-mrad field with a 1.7-mrad (1/10°) receive field-of-view. This is accomplished electronically by scanning the largest aperture in the image-dissector tube. When each satellite has detected the laser signal of the other satellite, it narrows its transmit beam from 17 mrad × 1.7 mrad to 1.7 mrad × 1.7 mrad. The received power increases by 17 dB, which greatly shortens the time required for the scans in the later steps. The transmit beam then remains fixed until the acquisition is complete, at which time it is narrowed further to a width of 400 mrad × 80 μrad. The second step of the acquisition is done with an instantaneous receiver field-of-view of 400 μrad, which is scanned electronically over a 1.7-mrad field until detection is made. The third step uses a 100-μrad receive field-of-view and the fourth step uses a 17-μrad (1/1000°) field-of-view. After the laser beam is detected with the smallest hole of the image-dissector, the satellite narrows its transmit beam and goes into the communication and tracking modes as soon as it detects, by a large increase in received signal level, that the other satellite has completed acquisition and has also narrowed its transmitted beam. A flow chart of the acquisition procedure is shown in Fig. 5.

The angle-stability requirements for the attitude-control system of the satellite are found to be 1-mrad peak excursion in 3 minutes and a maximum drift rate of 50 μrad/sec.

38
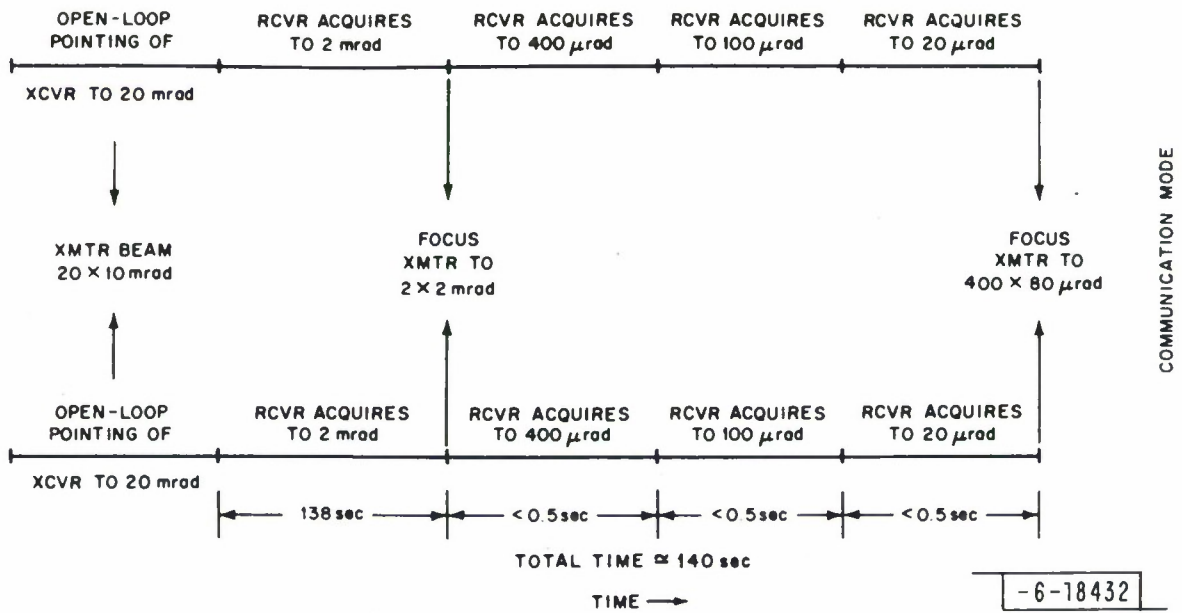
Fig. 5. Acquisition Procedure for 4-FOV System.

B. Some Practical Considerations

In this section we consider some side issues of the optical acquisition problem, which are of considerable practical importance. We shall discuss various types of scan patterns, the use of overlapping search FOVs when platform instability is important, searching in the time domain as well as in angle when the source is pulsed, and transmitter search strategies used in conjunction with the receiver FOV strategies discussed earlier. Finally, we give an example of a combined transmitter/receiver strategy applied to a very-narrow-beam optical communication system in which the transit time of light and the relative motion of the satellites causes the familiar "point-ahead" effect.

1. Scan Patterns

If one assumes that the probability density of the position of the source is uniform over a bounded acquisition field-of-view (AFOV), and if the position of the source does not change during the search, then the acquisition time is the same for all scan patterns covering the AFOV. However, the various scan patterns differ in case of implementation and have different properties when the source does move during the search, or the source is more likely to be, for example, in the center of the AFOV.

The following three scan patterns should be considered:

a. Linear Scan: The instantaneous FOV moves in a TV-like raster with or without flyback.

b. Direct Spiral Scan: The scan starts in the middle and winds its way out continuously. Alternatively one could have a reverse spiral, starting at the outside.

c. Pseudo-Random Scan: No apparent order to scan; however, at the end of the scan the whole AFOV has been searched once and only once.

In general, one might expect the source to be near the middle of the acquisition FOV, rather than near the edge. The probability density function of the source position would then be monotonically decreasing from the center of the AFOV. In this case the average acquisition time (but not the maximum) can be reduced by using a (direct) spiral scan rather than a linear or random scan.

In another kind of practical situation, the AFOV may not be bounded. For such a case one may define an AFOV with will contain the source with high probability. It will occasionally happen that the source is initially outside the AFOV so defined. When this occurs, the satellite telescope must be repointed.

2. Acquisition in Time as Well as Angle

Determining the time of arrival of a pulsed signal is theoretically equivalent to acquiring in angle. The implementation, however, is quite different. If detection can be made on a single pulse, then one is essentially forced to examine each time position sequentially, i.e., perform a linear scan. If detection can only be accomplished by integration over many pulses of a pulse train, then one can do parallel processing, and the important question is how long one must integrate to detect reliably.

If one is searching in both time and angle, then the treatment is less straightforward. If one were doing a linear scan in angle over the AFOV, and if detection could be made on a single pulse, the total number of search positions would be

41

$$M = \frac{A_o}{A_f} \quad * \quad \frac{T_o}{T_f} \tag{62}$$

where T_o is the pulse period and T_f is the pulse length. The total number of bins to be searched is the product of the number of time bins and the number of angle bins.

On the other hand, if one does a binary angular scan with check, then it is very simple to determine the time-of-arrival of the pulsed signal in the first step of the angle acquisition. Similar considerations hold for the combined scan techniques, such as the receiver with four apertures.

3. Transmitter Beam Strategies

Another possible strategy is to scan the optical transmitter on satellite A, while the receiver at satellite B has a sufficiently wide FOV to guarantee that the signal will be seen. This is equivalent to the acquisition problem studied in the body of this paper. This assumes, of course, some way of relaying the fact of a detection back to the transmitter. In fact, implementation of multiple transmitter beam sizes (instead of multiple receiver FOVs) can be achieved by mechanical, acoustical-optical or electro-optical techniques.

If one scans both the transmitter and the receiver, the issues (as in the time vs angle case) are less straightforward. Consider the quantum-noise-limited case. Assume the receiver gets λ photons/sec if the transmit beam is focused to θ_f, the final desired angular uncertainty. It would receive $\frac{\lambda}{M}$ photons/sec (where $M = \frac{\theta_o^2}{\theta_f}$) if the transmit beam were defocused to cover the total angular uncertainty, θ_o. If T is the integration (or dwell) time the receiver uses when the transmit beam is collimated, then MT is the dwell

42

time if the transmit beam is defocused. If the transmit beam is collimated, it must sequentially scan the M possible angular positions. Thus the total acquisition time is the same in either case.

The collimated transmit beam could be advantageous in two circumstances. First, its use gives shorter receiver scan times for each position of the transmit beam, and therefore platform-stability requirements may be significantly relaxed. Secondly, the threshold effect of background and receiver noise can lead to reduction of the total acquisition time. By using a small-enough transmit beam, one can increase the signal level enough to almost guarantee quantum-noise-limited detection when the signal source is in the receiver AFOV.

In the foregoing we have assumed one-way communication, in the following sense. Satellite A has a beacon with a fixed beam size, while B has a receiver and a transmitter. Its receiver acquires the beacon in order to obtain pointing information for its narrow transmit beam, which it uses for data communication. Thus the communication is from satellite B to satellite A.

If two-way communication is required, then satellite A must acquire the transmit signal from satellite B. However, this signal is right on target, and therefore the acquisition of the second communication link is very rapid.

The two links can be acquired together, rather than sequentially. Thus, every time satellite B narrows its receiver FOV, it would narrow its transmitter beam accordingly.

Consider, for example, the case where both satellites do a binary scan with check. Let $M = 2^{20}$ ($\approx 10^6$), and the initial integration time be T.

The acquisition time will be $T_a = 2T + 2T/2 + 2T/4 + \ldots + 2T/2^{20}$ (20 terms).

$$T_a \approx 4T \text{ (within 1 ppm)}$$

With a simple binary scan the total time would have been

$$T_a = 2T \log_2 M = 40T \quad .$$

In fact, the maximum scan time for the duo-binary scan is virtually independent of M for $M \geq 8$

$$T_a = \left\{ 4T \ 1 - (1/2)^{1+\log_2 M} \right\} \quad . \tag{23}$$

Now consider the background-noise-limited case where the background noise is much larger than signal $\left(\dfrac{n_S}{n_B} \ll 1 \right)$ even when the transmitter is well-collimated and when the receiver uses its narrow FOV. One presumably would not want to design a communications system like this, although with a deep-space probe one might have to. However, the analysis is much simpler and allows one to draw more interesting conclusions.

We want to compare three situations:

1. The transmitter beam remains defocused throughout the receiver binary acquisition.

2. The transmitter beam is collimated throughout the receiver binary acquisition and does a linear scan.

3. The transmitter beam does a binary reduction in step with the receiver binary search.

In the quantum-noise-limited case we found that 1 and 2 were equivalent and that 3 was superior to 1 and 2 by a factor $\log_2 M$. In the background-noise-limited case we shall find that 2 is superior to 3, which, in turn, is

44

comparable to 1. That is, one does best in the noisy case by making the transmit beam as narrow as possible.

Under the assumption of background-noise-limited, operation, the integration time T, from Eq. 55, is given by

$$T = \frac{K_o \lambda_n}{\lambda_s^2} \quad,$$

$$K_o = \left[2\sqrt{C} + \sqrt{C - 1 + \ln M} \right]^2 \tag{64}$$

λ_s = signal photon arrival rate

λ_n = noise photon arrival rate for largest FOV

Given the general expression for the integration time T we calculate the receiver acquisition time for the binary case. At each step the noise reduces by a factor of 2. $T_A(\text{binary}) = T_1 + T_2 - T_{\log_2} M$

$$T_1 = \frac{K_o \lambda_n}{\lambda_s^2}$$

$$T_2 = \frac{K_o \frac{\lambda_n}{2}}{\lambda_s^2}$$

$$T_i = \frac{K_o \frac{\lambda_n}{2^{i-1}}}{\lambda_s^2}$$

$$T_A = \frac{K_o \lambda_n}{\lambda_s^2} \sum_1^{\log_2 m} (\tfrac{1}{2})^{i-1} = \frac{K_o \lambda_n}{\lambda_s} 2\left(1 - (1/2)^{\log_2 m}\right)$$

$$= \frac{K_o \lambda_n}{\lambda_s^2} 2(1 - \frac{1}{M}) \approx \frac{2 K_o \lambda_n}{\lambda_s^2} \tag{65}$$

45

The receiver acquisition time for the linear scan is simply $M \cdot T$:

$$T(\text{Linear}) = \frac{M \, K_o \, \lambda_n}{\lambda_s^2} \tag{66}$$

If λ_s is the arrival rate for the defocused transmit beam, then $\lambda_s M$ is arrival rate for the collimated beam. Assume that the receiver and transmitters are similar on the two satellites.

We first calculate the total acquisition time (T_{total}) for the case in which the transmit beam on satellite A remains defocused throughout the scan, and the receiver on B does a binary search. We have:

$$T_{Total} = \frac{K_o \, \lambda_n}{\lambda_s^2} \, 2(1 - \frac{1}{M}) \tag{67}$$

$$\approx 2 \, \frac{K_o \, \lambda_n}{\lambda_s^2}$$

We then calculate case 2 where the transmit beam is collimated throughout the receiver acquisition and does a linear scan.

$$T_{Total} = M \times T_a \quad \text{(for each transmit position)}$$

$$= M \times \frac{K_o \, \lambda_n}{(M\lambda_s)^2} \, 2(1 - \frac{1}{M}) \tag{68}$$

$$T_{Total} = \frac{K_o \, \lambda_n}{\lambda_s^2} = \frac{1}{M} \, 2(1 - \frac{1}{M})$$

$$\approx 2 \cdot \frac{1}{M} \cdot \frac{K_o \, \lambda_n}{\lambda_s^2} \tag{69}$$

46

Case 3 is the duo-binary situation in which the transmitter reduces its beam by a factor of 2 each time the receiver reduces its FOV by 2.

$$T_{Total} = T_1 + T_2 + T_{\log_s M}$$

$$T_1 = \frac{K_o \lambda_n}{\lambda_s^2} \quad \text{from Eq. B,} \tag{70}$$

In the second step the noise is reduced by 2 and the signal increased by 2, thus,

$$T_2 = \frac{K_o(\lambda_{n/2})}{(2\lambda_s)^2} = \frac{K_o \lambda_n}{\lambda_s^2} \times 1/8$$

$$T_i = \frac{K_o \lambda_n}{\lambda_s^2} (\tfrac{1}{2})^{3(i-1)}$$

Then,

$$T_{Total} = \sum_{i=1}^{\log_2 m} T_i = \frac{K_o \lambda_n}{\lambda_s^2} \sum_{i=1}^{\log_2 m} (\tfrac{1}{2})^{3(i-1)}$$

$$= \frac{K_o \lambda_n}{\lambda_s^2} \left[\frac{1-(1/8)^{\log_2 m}}{1-(1/8)} \right]$$

$$T_{Total} \approx \frac{8}{7} \left\{ \frac{K_o \lambda_n}{\lambda_s^2} \right\} \tag{71}$$

Thus we see that, for the case of very high background noise, the duo-binary procedure is slightly better than the spread-transmit-beam procedure. The scanned collimated transmitter is far superior, with total acquisition time shorter by a factor of M.

Inspection of the series which yields the total acquisition time for the spread-beam case, and for the duo-binary case, reveals that the sum is dominated by the first few terms. In both cases, the first term is the same, namely, the integration time for a spread transmit beam. Thus one expects the sums to be comparable.

4. Compensation of Point-Ahead Errors in Satellite-to-Satellite Optical Communication

As an application of the multiple FOV acquisition consider the following very special system which is motivated by an early system-design problem considered by NASA. Two satellites communicating with each other with light beams must offset their transmitted beams, in general, from the received signal direction (i.e., they must "point ahead"). The magnitude of this effect, which varies with the transverse component of relative velocity between the satellites, can be important; for example, if it is of the order of 50 μrad, it is large compared to the optical beamwidth necessary for high-data-rate applications.

Of the two basic philosophies for compensation of these errors (viz, real-time computation and prediction of offset angles, or modified active tracking), the second is more desirable from the standpoints of conceptual simplicity, hardware economy, and ease of implementation. The computation option would require precise determination by some means of the orbits of both satellites, with a computer somewhere (in orbit or on the ground) to calculate the corrections, and open-loop pointing systems sufficiently accurate and stable to make and maintain the corrections. If the pointing systems were closed-loop they would essentially be active trackers, which could just

48

as well have been realized in the simple non-predicting configuration proposed in this note.

The active-tracking scheme depends in general upon separate control of the receiver and the transmitter on the same satellite. The receiver tracks the incoming signal direction in a conventional manner, while the transmitter is controlled in response to pointing-angle error signals based upon received-power data measured at and sent back from the other satellite. Because of this dichotomy, initial acquisition is considerably more complex than in the conventional situation. The approach described here begins with defocused transmitter beams, thereby minimizing acquisition time and avoiding mechanical beam-scanning.

The particular configuration to be considered has a 1 gigabit/sec laser transmitter and a tracking receiver on a low-orbit satellite (L), with a tracking/communications receiver and a low-power beacon transmitter on a synchronous-orbit satellite (S).* The altitude of satellite (L) is 160 km, and its period is about 90 minutes. In general, satellite (L) will disappear behind the earth for some fraction of each orbit, as viewed from satellite (S). When it reappears, it will be visible above the horizon for a minimum of 6.3 minutes, before it begins to move across the disk of the earth. Acquisition must be accomplished during this time, because it is essentially impossible with the brightly-sun-lit earth as a background; the acquisition time would be long compared to the orbit period. (Communication with the earth as background is easy; with a 5 μrad receiver beam, the signal-to-noise ratio is +71 dB.)

---

*Such a situation may exist on NASA's LANDSAT, where they plan to handle 10,000 photographic images per week to determine agricultural growth patterns.

For the assumed set of orbit parameters the point-ahead error is upper-bounded by about 50 μrad. This is 10 times greater than the XMTR beamwidth of satellite (L), which has a 1 W Nd:YAG laser (its characteristics are listed in the following section of this note). Satellite (S) does not need point-ahead compensation, because its beacon XMTR beamwidth is large compared to 50 μrad (its beacon is assumed to be one pulsed GaAlAs diode laser, similar in numerical parameters to those in the LES-8/9 XCVR, with 6-inch optics and a 500 μrad minimum transmit beam size).

The following table lists the steps in a credible acquisition procedure, which is subsequently explained in more detail. The apparent complexity of the table is a consequence of the interplay of signal-strength, background-noise and angular-drift-rate limitations, which can be only partially circumvented at each step of the process. It should be noted that this is only one of a class of possible schemes which flow in a smooth logical progression through final acquisition. Table 1 graphically summarizes the procedure.

In Step 1 it is assumed that satellite (S) can aim its receiver a priori to within ± 10 mrad of the point at which satellite (L) will appear over the horizon. The receiver beam will be held just above the horizon as it scans ± 10 mrad (using a multi-aperture image-dissector photomultiplier tube), until the target is detected as it crosses the scan line. The figure of 9.76 sec, derived below, is an upper bound on the required scan time. Step 2 is a conventional search over the resulting 2 mrad region of uncertainty. The receiver acquisition cannot proceed further at this point, because the 500 μrad beamwidth is comparable to the motion of the target during one integration time.

50

Step 3 is self-explanatory; knowing the location of satellite (L) to within 500 μrad, satellite (S) narrows its XMTR beam to that width, thereby making it possible for the other satellite to acquire within a reasonable time interval. Step 4 is the culmination of a scan which has been going on since the beginning of Step 1, but could not be successful until Step 3 was completed. After Step 5 the integration time for satellite (S) is short enough that angular drift is no longer a problem, and Step 6 can be carried out very quickly.

Step 7 (which has actually been going on in parallel with Steps 5 and 6) is directed toward minimizing the angular region of uncertainty for the XMTR scan of Step 8. There is no reason to decrease the RCVR beam below 100 μrad at any later stage. Step 8 involves scanning 400 XMTR beam positions, for each of which the dwell time is 7.5 nsec. The speed of this step is controlled by equipment limitations (since the scanning must be done electro-optically or mechanically), and is also influenced by the round-trip delay from satellite (L) to (S) and back, which is approximately 0.25 second. Thus, when satellite (L) receives a message from (S) that it is now aimed so as to maximize received power at (S), it must immediately back up one-quarter second in its scan, and must then put the final trim on its direction of aim.

Subsequent tracking is carried on in the usual manner by the RCVR in satellite (S), and analogously by the XMTR of satellite (L) (e.g., the XMTR steps through a small cruciform scan and obtains received-power figures from (S) one-quarter second later). Because of their broad beams, both the XMTR in (S) and the RCVR in (L) can be simply slaved to their respective partners on board.

Assumptions and Calculations

1. Assumptions

    a.   Source on low satellite (L):   Nd:YAG

          Wavelength: 1.06 µm

          Transmit power: 1 watt

          Loss in optics: 6 dB

          Transmit beamwidth:

              i.   20 mrad

            ii.   2 mrad

           iii.   5 µrad

    b.   Range: 42,500 km

    c.   Receiver on synchronous satellite (S):

          Detector: image-dissector tube, new photocathode

          Bandwidth: 0.1 nm

          Quantum Efficiency: 0.01

          Photon Energy: $h\nu = 1.87 \times 10^{-19}$ joule

          Assumed dark current in 20 mrad FOV: 10^4 ph el/sec

          Stellar Background in 20 mrad FOV: Equivalent of 300 MAG 10 stars or 400 ph el/sec

          Objective lens diameter: 15 cm

          Receiver area: 0.0175 m^2

          Receiver field of view:

            optical: 20 mrad

            image dissector: (i)   2 mrad

                                  (ii)   500 µrad

                                  (iii)   50 µrad

                                  (iv)   5 µrad

d. Relative drift rate ≈ 75 μrad/sec

e. Source on synchronous satellite (S): GaAlAs diode

Wavelength: 900 nm
Transmit power: 4 watts peak
Loss in optics: 6 dB
Pulse length: 100 nsec
Pulse-repetition   3,000/sec
    frequency
Transmit beamwidth: (i)   20 mrad square
                     (ii) 500 μrad square

f. Receiver on Low Satellite (L)

Detector: Image-dissector PMT with two FOV's

Quantum Efficiency: 0.03

Bandwidth: 5 nm

Photon energy: 2.22×10^{-19} joule

Objective lens diameter: 15 cm

Objective lens area: 0.0175 m^2

Receiver field-of-view: Optical: 20 mrad
                         Image dissector:

                         (i)   2 mrad
                         (ii) 100 μrad

Assumed dark current in 20 mrad FOV: 5×10^3 ph el/sec

Stellar background level in 20 mrad FOV: 5×10^3 ph el/sec

Stellar background level in 100 μrad FOV: ~ 0.13 ph el/sec

2. Received Nd:YAG Signal Level

$$S = \frac{4}{\pi} \frac{\eta}{h\nu} \frac{P_T A}{R^2 \beta_t^2}$$

where S = photoelectrons/sec

            η = quantum efficiency

            $h\nu$ = energy of a photon

            P_T = effective transmit power

$$A = \text{receiving aperture area}$$
$$R = \text{range}$$
$$\beta_T = \text{transmit beamwidth}$$

For a 20 mrad transmit beamwidth

$$S = \frac{4 \times 10^{-2} \, (\frac{1}{4}) \quad 1.75 \times 10^{-2}}{\pi 1.87 \times 10^{-19} (4 \times 10^{7})^{2} (2.0 \times 10^{-2})^{2}}$$

For a 2 mrad transmit beam

$$S = 4.65 \times 10^{4} \text{ ph el/sec}$$

For a 5 μrad transmit beam

$$S = 7.45 \times 10^{9} \text{ ph el/sec}$$

Earth Background Noise

  Assumptions:

    Lambert's Law reflection
    Albedo of 100%
    Satellite FOV small compared to earth

Corresponding spectral radiance of Earth $B = \frac{K_s}{\pi}$ W/(m^2 $-$ sr $-$ μm), where K_s is the solar spectral irradiance in W/m^2 $-$ μm.

  Received power on satellite is

$$P_R = B \Omega_R A_R W_R \quad ,$$

where Ω_R and A_R are the beam solid angle and aperture area of the satellite receiver, respectively, and W_R is the optical bandwidth of the receiver. Let $\Omega_R = K_d \Omega_d$, where Ω_d is the diffraction-limited beam size of the receiver; then

54

$$P_R = \frac{K_s K_d \pi \lambda^2 W_R}{16} \qquad .$$

Assume $K_s W_R = 0.1$ watt/m^2 (0.1 nm filter); then the noise photoelectron rate B_E is

$$B_E = \frac{\eta}{h\nu} P_R \overset{\sim}{=} 590 \ K_d \ \text{ph. el./sec, for Nd:YAG parameters.}$$

Consider two limiting cases:

1. First step of acquisition

    Nd:YAG beamwidth 20 mrad (S = 465 ph.el./sec)

    Satellite (S) receiver beamwidth 2 mrad

    $$K_d = (400)^2 \ \text{(diffraction-limited beamwidth} \sim 5 \ \mu\text{rad)}$$

    $$\therefore \quad B_E = 590 \times 1.6 \times 10^5 \overset{\sim}{=} 9.44 \times 10^7$$

    Signal-to-noise ratio $S/B_E = 4.93 \times 10^{-6} \rightarrow -53$ dB

    $$\therefore \quad \text{acquisition impossible with Earth background.}$$

2. Communication mode:

    Nd:YAG beamwidth 5 μrad (S = 7.45×10^9 ph.el./sec)

    Satellite (S) RCVR beamwidth 5 μrad ($K_d = 1$)

    $$B_E = 590 \ \text{ph.el./sec}$$

    $$S/B_E = 1.26 \times 10^7 \rightarrow +71 \ \text{dB}$$

    $$\therefore \quad \text{Earth background insignificant for communication mode.}$$

Acquisition Time -- Step 1

From Ref. 6*

$$P(E) \leq \exp[-S\tau Q(S/B)]$$

which is set to about $10^{-4} \approx e^{-10}$. Background B is 100 ph.el./sec. in 2 mrad FOV. Thus

$$S/B = 4.65 \qquad (+6.7 \text{ dB})$$

and

$$Q(+6.7 \text{ dB}) = 0.22$$

The integration time is

$$\tau = \frac{10}{465 \times 0.22} = .0976$$

$$\tau = 97.6 \text{ msec}$$

There are 10×10 steps, which makes the scan time 9.76 seconds.

Acquisition Time -- Step 2

Search with 500 μrad F.O.V.; background

$$B = 6.6 \text{ ph.el./sec.}$$

---

*Here we inappropriately use the analysis for a binary decision rather than the appropriate analysis in the M-ary decision case for which we later developed a graphical solution method. We believe the concepts are quite valid and that the calculated times are approximately correct.

Thus

$$S/B = 18.79 \text{ dB and } Q(18.7 \text{ dB}) = 0.45$$

$$\tau = \frac{10}{465 \times (0.45)} = 47.5 \text{ msec}$$

For 16 positions, a 760 msec scan time is required.

Acquisition Time -- Step 4

Search with 2 mrad FOV for GaAs beacon. Assume same parameters as for LES-8/9 GaAs link except area of optics is smaller by 1/4 and only one diode operated at 3 kHz instead of 10 operated at 30 kHz. From LES-8/9 calculations it was found that the dwell time for one position with 2 mrad transmit beam and a 2 mrad receiver FOV was 7.8 msec. Thus a 500 μrad transmit beam (factor-of-16 increase) together with the factor-of-$(\frac{1}{40})$ decrease mentioned above make the dwell time $\frac{40}{16} \times 7.8 = 19.4$ msec. There are 10×10 positions to be searched, making the scan time 1.94 seconds.

Acquisition Time -- Step 6

Synchronous satellite acquires Nd:YAG signal with 50 μrad FOV from field of 500 μrad with transmit beam of 2 mrad. There is a 20 dB increase in received signal and a 20 dB decrease in background, causing a 40 dB increase in signal to background ratio over step 2, thus making S/B = 58.7 dB. Q(58.7 dB) 0.7. The integration time is

$$\tau = \frac{10}{4.6 \times 10^4 \times 0.7} = 3.08 \times 10^{-4}$$

$$\tau = 0.308 \text{ msec}$$

The 100 positions therefore require 30.8 msec.

The next part of this step requires scanning with a 5 μrad FOV. This scan also requires 30.8 msec since the Q function increases very slowly for increasing S/B.

Acquisition Time -- Step 7

Low satellite acquires fully collimated GaAs beam with 100 μrad FOV. The dwell time is approximately (see step 4) 19.4/7.8 = 2.5 msec, giving a scan time of $20 \times 20 \times 2.5 = 1$ sec.

Acquisition Time -- Step 8

Here the Nd:YAG transmitter scans with its 5 μrad beam over a 100 μrad field. The dwell time is $(200)^2$ faster than that for step 6, making it 7.5 nsec. The minimum scan time is $20 \times 20 \times 7.6 = 3$ μsec. The Nd:YAG transmitter will stop scanning after it receives a signal from the Nd:YAG receiver to do so. This signal has a round-trip transit time of 0.25 sec. The scan could be done electro-optically at sweep rates of abou 10 kHz. Thus a conservative total scan time estimate is given at 1 second.

TABLE II

ACQUISITION PROCEDURE

Satellite (S)	Satellite (L)	Time
1. Acquire with 2 mrad RCVR beam over ±10 mrad on limb of earth.	XMTR beam stationary, width 20 mrad.	9.76 sec
2. Acquire with 500 μrad RCVR beam over 2 mrad field.		0.76 sec.
3. Collimate XMTR beam to 500 μrad (RCVR tracks)		
4.	Acquire with 2 mrad RCVR beam over 20 mrad field.	1.94 sec
5. (RCVR notes a 20-dB increase in received power.)	Collimate XMTR beam to 2 mrad	
6. RCVR acquires first to 50 μrad, then to 5 μrad, over 500 μrad field.		62 msec
7. RCVR tracks and is ready for communication mode	RCVR acquires to 100 μrad, over 2 mrad field	1.0 sec
8.	Correct XMTR pointing by collimating to 5 μrad, then scanning over 100 μrad field.	∿1.0 sec
9. Both satellites in full communication mode.		
	Total Time	∿14.5 sec

TABLE III

PARAMETERS ASSUMED FOR SATELLITE-TO-SATELLITE OPTICAL COMMUNICATION SYSTEM

<u>Transmitter</u>

Source:	GaAs diode laser array
Wavelength:	$0.9~\mu m(9,000~\overset{\text{o}}{\text{A}})$
Transmit Power:	4 watts peak
Loss in Optics:	6 dB
Transmit Pulse Duration:	100 nsec
Transmit Pulse Energy:	10^{-7} joule
Pulse Repetition Frequency:	31,250 pulses/sec
Coding:	4 Bit Pulse Position Modulation (PPM)
Data Rate:	125 kB/sec

Transmit Beamwidths:

- a)   17.45 mrad x 17.45 mrad
- b)   2.2 mrad x 2.2 mrad
- c)   100 µrad x 300 µrad

<u>Receiver</u>

Detector:	Image-Dissector with 4 FOVs
Quantum Efficiency:	0.03
Tube Diameter:	2.5 cm
Objective Lens Diameter:	30 cm
Objective Lens Area:	$0.07~m^2$

TABLE III (cont'd.)

Receiver (cont'd.)

Dark Current: Expected: $20{,}000/\text{cm}^2 + 20$ ph. el./sec

Background Level: 20,000 ph. el./sec over 17.45 mrad FOV, or 83.6 ph. el./sec per $(\text{mrad})^2$

2×10^4 ph. el./sec

Aperture Sizes: A_1: 2.2 mrad square FOV

A_2: 436 µrad square FOV

A_3: 87.3 µrad square FOV

A_4: 17.45 µrad square FOV

Receiver Optical Bandwidth: 5 nm

Range 4×10^7 m

Received Signal Levels:

     a)   With 17.45 mrad x 17.45 mrad transmit beam: 1.94×10^{-3} ph. el./pulse

     b)   With 2.2 mrad x 2.2 mrad beam: 0.122 ph. el./pulse

     c)   With 100 µrad x 300 µrad beam: 19.7 ph. el./pulse

TABLE IV

COMPARISON OF MAXIMUM SCAN TIMES FOR VARIOUS MULTIPLE FIELD-OF-VIEW RECEIVERS FOR SATELLITE-TO SATELLITE OPTICAL COMMUNICATION SYSTEM

	2 (Binary Search)	$e = 2.718$	3	6	32	100	1000	10^6 (Raster Scan)
Ratio of Successive FOVs α								
Number of FOVs n_α	20	14	13	8	4	3	2	1
Maximum Acquisition Time T_a (seconds)	4.1×10^{-1}	3.9×10^{-1}	4.0×10^{-1}	4.9×10^{-1}	1.3	3.09	20	1.03×10^4 (2.8 hrs.)
Time Relative to Optimum	1.05	1.00	1.026	1.25	3.33	7.92	51	2.6×10^4

TABLE V

PARAMETERS OF FOUR-APERTURE PHOTOMULTIPLIER TUBE

Photocathode Diameter: 1.0 inch

Radiant Sensitivity: 10 mA/W and

                                25 mA/W, both at 850 nm wavelength
                                (quantum efficiencies 1% and 3%,
                                respectively)

Dark Current: $\leq 10^3$ photoelectrons per second

                                per cm^2 of photocathode area

Resolution with 0.001-inch aperture: 0.001 inch at photocathode center

                                0.005 inch 0.4 inches from cathode-
                                center

Gain: $\geq 10^6$

Physical Dimensions: Diameter, tube alone: $\leq$ 1.6 inch

                                Diameter with deflection $\leq$ 3.5 inches
                                coils:

                                Length: $\leq$ 9.0 inches

REFERENCES

1. Proc. of the IEEE, Special Issue on Optical Communications (October 1970).

2. W. K. Pratt, <u>Laser Communication Systems</u> (J. Wiley and Sons, 1969).

3. R. E. Johnson and P. F. Weiss, "Laser Tracking System with Automatic Reacquisition Capability," Appl. Opt. <u>7</u>, 1095-1102 (1968).

4. D. E. Knuth, <u>Sorting and Searching</u>, Vol. 3 of <u>The Art of Computer Programming</u> (Addison-Wesley Publishing Co., Cal., 1973) (Section 6.2.2, "Binary Tree Searching").

5. R. M. Fano, <u>Transmission of Information</u> (MIT Press and J. Wiley & Sons, N. Y., 1961).

6. E. A. Bucher, "Error Performance Bounds for Two Receivers for Optical Communications and Detection," Appl. Opt. <u>11</u>, 884-889 (1972).

GLOSSARY OF ACRONYMS AND ABBREVIATIONS

FOV	Field of View
M	Total number of positions to be searched
n	Number of searches (different FOV's)
n_o	Optimum value of n
A_o	Designates initial search area (designates acquisition FOV)
A_1	Search FOV #1, instantaneous FOV #1
A_f	Final FOV
T	Integration time for a single position
P_m	Probability of a miss (not detecting a signal when there is one present)
λ	Rate parameter of Poisson signal
T_a	Maximum acquisition time
α_i	A ratio of FOV's
γ	Lagrange variable
e	Base of the natural logarithm
v_i	Velocity of a FOV
τ	Unit of time
u_i	A distance
ρ_i	A time
ϕ_i	A distance
θ	A time
T_s	Total scan time
L	A distance

Δ	A time
τ_t	A pulse width in time
f_s	Signal repetition rate
cW	Continuous wave
n_s	Signal counts
n_G	Background counts
K_0	Constant
λ_n	Noise photon rate
λ_s	Signal photon rate

SECURITY CLASSIFICATION OF THIS PAGE *(When Data Entered)*

REPORT DOCUMENTATION PAGE		READ INSTRUCTIONS BEFORE COMPLETING FORM
1. REPORT NUMBER ESD-TR-77-224	2. GOVT ACCESSION NO.	3. RECIPIENT'S CATALOG NUMBER
4. TITLE *(and Subtitle)* Spatial Acquisition in Optical Space Communications		5. TYPE OF REPORT & PERIOD COVERED Technical Note
		6. PERFORMING ORG. REPORT NUMBER Technical Note 1977-19
7. AUTHOR*(s)* Alvise A. Braga-Illa Estil V. Hoversten Harold M. Heggestad John T. Lynch		8. CONTRACT OR GRANT NUMBER*(s)* F19628-76-C-0002
9. PERFORMING ORGANIZATION NAME AND ADDRESS Lincoln Laboratory, M.I.T. P.O. Box 73 Lexington, MA 02173		10. PROGRAM ELEMENT, PROJECT, TASK AREA & WORK UNIT NUMBERS Program Element No. 63431F Project No. 1227
11. CONTROLLING OFFICE NAME AND ADDRESS Air Force Systems Command, USAF Andrews AFB Washington, DC 20331		12. REPORT DATE 6 September 1977
		13. NUMBER OF PAGES 76
14. MONITORING AGENCY NAME & ADDRESS *(if different from Controlling Office)* Electronic Systems Division Hanscom AFB Bedford, MA 01731		15. SECURITY CLASS. *(of this report)* Unclassified
		15a. DECLASSIFICATION DOWNGRADING SCHEDULE

16. DISTRIBUTION STATEMENT *(of this Report)*

Approved for public release; distribution unlimited.

17. DISTRIBUTION STATEMENT *(of the obstract entered in Block 20, if different from Report)*

18. SUPPLEMENTARY NOTES

None

19. KEY WORDS *(Continue on reverse side if necessary and identify by block number)*

Optical Communications   LES-8/9   signal-to-noise ratio

20. ABSTRACT *(Continue on reverse side if necessary and identify by block number)*

Early in 1972 Lincoln Laboratory made the decision to discontinue the development effort for an Optical Communications link between LES-8 and LES-9. The opportunity to document our early effort never seemed to come. Now, 5 years later, after the launch of LES-8/9, it seems worthwhile to write down some of our thinking on what turned out to be an intriguing problem. Two of the four collaborators are now distantly located and involved in other pressing problems so that it is not possible to write a paper as complete as we would have liked. Here is a slightly edited version of the acquisition analysis we did. Omitted are the interesting but incomplete results for the case of moderate signal-to-noise ratio.

DD   FORM 1473   EDITION OF 1 NOV 65 IS OBSOLETE
1 JAN 73

SECURITY CLASSIFICATION OF THIS PAGE *(When Dato Entered)*